UC Irvine
UC Irvine Previously Published Works

Title
Assessment of the regional fossil fuel CO2 distribution through ∆14C patterns in ipê leaves: The case of Rio de Janeiro state, Brazil

Permalink
https://escholarship.org/uc/item/7x50z5s4

Authors
Santos, Guaciara M
Oliveira, Fabiana M
Park, Junghun
et al.

Publication Date
2019-09-01

DOI
10.1016/j.cacint.2019.06.001

Peer reviewed

eScholarship.org Powered by the California Digital Library
University of California

City and Environment Interactions 1 (2019) 100001

Contents lists available at ScienceDirect

City and Environment Interactions

journal homepage: www.elsevier.com/locate/cacint

Assessment of the regional fossil fuel CO_2 distribution through $\Delta^{14}C$ patterns in ipê leaves: The case of Rio de Janeiro state, Brazil

Guaciara M. Santos [a,*], Fabiana M. Oliveira [b], Junghun Park [c], Ana C.T. Sena [a], Júlio B. Chiquetto [d], Kita D. Macario [b], Cassandra S.G. Grainger [a,e]

[a] Department of Earth System Science, University of California, Irvine, USA
[b] Institute of Physics, Universidade Federal Fluminense, Niterói, Brazil
[c] Korea Institute of Geoscience and Mineral Resources, Geochemical Analysis Center, Daejeon, South Korea
[d] Institute of Advanced Studies, University of São Paulo, Sao Paulo, Brazil
[e] Public Library of Science journal, San Francisco, USA

ARTICLE INFO

Article history:
Received 6 February 2019
Received in revised form 15 May 2019
Accepted 19 June 2019
Available online 26 June 2019

Keywords:
Ipê leaves
Stable isotope analysis
Radiocarbon
Fossil fuel emissions
GHG inventory

ABSTRACT

Fossil fuel-derived CO_2 (Cff) emission patterns and their point sources across the Rio de Janeiro megacity and state were estimated from a single regional-scale $\Delta^{14}C$ distribution map based on isotopic measurements of ipê leaves (*Tabebuia*, a popular flowering deciduous perennial tree). Data from multi-year sampling (i.e., 2014–2016) was renormalized to reflect ^{14}C signatures of the 2015 calendar year. Spatial variability in $\Delta^{14}C$ ranges from a maximum of 27.1 ± 0.4‰ (city of Petrópolis, a higher-elevation municipality) to a minimum of −43.6 ± 1.4‰ (i.e., approximately 27.6 ± 1 ppm of Cff — Santo Cristo, a district within the Rio de Janeiro city). Overall, higher $\Delta^{14}C$ values correlate well with green habitats and high elevation areas, while lower values are associated with Cff emissions in densely populated areas with higher industrial and traffic footprints. Cff emissions are higher where local air circulation is poor, such as the area surrounding Guanabara Bay. Other areas with significantly higher Cff emissions were the Paraíba Valley and Mountain regions. These results may be explained by atmospheric transport of CO_2 from neighboring states, such as São Paulo and Minas Gerais, and by the predominant west winds and the limited regional air flow created by large topographic features. Lower Cff emissions were observed in the Northwest and Lakes regions, which are dominated by agriculture and tourism activities. Our results highlight the potential of directly estimating Cff for studying urban landscapes in the southern region of Brazil through ^{14}C time-integrated distribution mapping of ipê leaves. The method could also be used to augment greenhouse gas (GHG) emissions inventory studies trends in partitioning Cff from CO_2 of bio-template sustainable sources.

1. Introduction

Researchers have confirmed that the continuing global rise in atmospheric CO_2 content is caused by anthropogenic CO_2 emissions [1]. Most of those contributions are associated with the burning of fossil fuels (coal, petroleum, and natural gas, among others). While many sources of CO_2 may have similar isotopic composition as the atmosphere itself, fossil fuel-derived CO_2 (Cff) is highly depleted in radiocarbon (i.e., $\Delta^{14}C = -1000‰$) and negative carbon isotopic signatures ($\delta^{13}C$ −28‰, in average) compared to cleaner air-CO_2 ($\delta^{13}C = -8‰$). Therefore, ^{14}C and carbon isotopic measurements of bottom-up point sources of air-CO_2 can improve our understanding of fossil fuel-derived CO_2 emissions in urbanized areas [2]. The isotopic effects due to Cff admixture on the C levels in air-CO_2 allow inferences into its overall emissions, and therefore can provide significant information that is helpful in establishing mitigation measures at the local, regional, and national levels.

Sophisticated studies (e.g. [3–9]) typically rely on higher-frequency or continuous measurements of trace gas concentrations (including CO_2 and CO), higher frequencies of measurements of ^{14}C in ambient air, and ancillary measurements of atmospheric dynamics (i.e., boundary layer height), or satellite observations of atmospheric column CO_2. In these studies, isotopic analysis is preferably carried out on air-CO_2 samples captured in pre-evacuated flasks [10,11], or zeolite molecular sieve traps [12]. Later, air-filled containers are shipped to laboratories for CO_2 extraction and cryogenic purification, so that specific isotopic measurements can be performed. Although these sampling methods are desirable, as they can better document the atmospheric isotopic changes, they can be challenging and extremely costly. They require special handling, distribution, and recovering of containers. Furthermore, suitable vacuum line systems for mass-production of CO_2 extractions are also necessary.

* Corresponding author at: Department of Earth System Science, University of California, Irvine, Irvine, CA, USA.
E-mail address: gdossant@uci.edu. (G.M. Santos).

http://dx.doi.org/10.1016/j.cacint.2019.06.001
2590-2520/© 2019 The Authors. Published by Elsevier Ltd. This is an open access article under the CC BY-NC-ND license (http://creativecommons.org/licenses/by-nc-nd/4.0/).

In regions where atmospheric observations are scarce or nonexistent, and therefore quantitative estimate emissions of Cff and other greenhouse gases cannot be easily attained, alternative approaches are required to estimate anthropogenic emissions. Besides conventional statistical inventory reports, plant tissue can be used to produce time-integrated records of $^{14}CO_2$ signatures that in turn can be translated into Cff mole fractions (ppm), which is relevant for stakeholders. Through photosynthesis, plants incorporate $^{14}CO_2$ from the local atmosphere into their biomass. Therefore, selected plant tissue layers from a single growing season can ideally be used to provide Cff information. Moreover, by using plant tissue as the primary material, the sampling logistics at the collection site and handling at the designated ^{14}C laboratory can be simplified and strengthened. In addition, its implementation is cost-effective, so this methodology can be applied to any areas where there are annually built-up layers of biological material. Obviously, plant growth takes time (months or weeks, at best). Consequently, the method can only derive an averaged characterization of the local fossil fuel CO_2. The method is also photosynthetic weight-limited, as CO_2 fixation occurs during daytime [13]. For meaningful isotopic comparisons and proper selection of plant species and their tissues/organs, some basic points on plant biology and physiology are also required. Plants, like many other living organisms, grow their tissues and organs at different rates. Thus, mixing those will lead to ^{14}C disequilibrium, large offsets [14], and possibly skewed results.

Similar short-growth plant-tissue ^{14}C datasets for evaluating Cff, with and without modeling analyses, have been developed across North America [15] and China [16] through corn leaves. Leaves of *Ginkgo biloba*, a deciduous type of tree considered sacred in eastern Asia, were used to provide snapshots and time-series of Cff over South Korea [17–19]. Radiocarbon analysis from individual maize plants (*Zea mays*) have provided information on both Cff and nuclear sources in the Netherlands during the years 2010 to 2012, and in western Germany and France in 2012, respectively [20]. Spatial and temporal reconstruction of Cff distribution and point sources have been investigated in grasses and wood in southern Italy [21]. To study CO and CO_2 pollution levels in urban ecosystems, Wang and Pataki [13] mapped ^{14}C distributions and the stable isotope parameters of ^{15}N, ^{18}O, ^{13}C, and C:N of C3 grasses in the Los Angeles Basin in 2004 and 2005. Using the ^{14}C values of annual C3 grasses, Riley et al. [22] produced an atmospheric transport model for the distribution and fluxes of atmospheric Cff across the state of California, USA.

To effectively mitigate anthropogenic atmospheric CO_2 in metropolitan areas, it is imperative to understand its magnitude, sources, and points of origin. The transport sector alone accounts for approximately 20% of global GHG emissions, according to the World Bank, and this figure is likely to be much higher in megacities, which concentrate many services and commerce. While it is impractical to directly monitor the CO_2 levels for every possible urban space, at the very least megacities (population of >10 million people) must be precisely monitored in order to evaluate progress toward mitigation goals [1]. Networks such as the NOAA/ESRL air sampling, paired with measurements of CO_2, CO, CH_4, N_2O, and SF_6, and a large suite of halocarbons and hydrocarbons (as mentioned by [9]), is a great example of such efforts.

Rio de Janeiro municipality and its surrounding cities are among the 55 urban areas worldwide which have already reached megacity status [23]. Rio de Janeiro state (RJ) lies in the southeastern region of Brazil, and together with the states of Espírito Santo, Minas Gerais, and São Paulo (Fig. 1), is responsible for approximately 60% of the Brazilian GDP and approximately 40% of the country's total population. This region also has the highest population density in Brazil (87 inhabitants/km^2), as well as the highest number of vehicles, industries, ports, and highways, among many other utilities. In accordance with the United Nations Framework Convention on Climate Change, Rio de Janeiro city has pledged significant greenhouse gas (GHG) emission reductions in comparison to 2005: several million tons of CO_2 equivalents (Mt CO_2e) by 2020. Reduction targets were defined as follows: 8% (0.93 Mt CO_2e) in 2012, 16% (1.86 Mt CO_2e) in 2016, and 20% (2.32 Mt CO_2e) in 2020 [24]. To achieve these goals, the city requires strengthening of local government actions, as well as efficient integration with state and federal-level environmental management policies, which must be implemented by policymakers. In RJ state, governmental inventory reports, such as SEEG-Brazil (The Greenhouse Gas Emissions and Removals Estimates) and GEE (Center for Integrated Studies on Climate Change and Environment), are still lacking in detailed CO_2 emission inventories data. Moreover, permanent air quality monitoring stations measuring tracer gases across the state are very scarce (e.g., [25]). Direct measurements of CO_2 data in RJMA also has been limited to distinct time periods – e.g., prior to the last FIFA World Cup in 2014 – and a handful of districts [26]. Therefore, independent quantitative estimates of CO_2 or Cff are still inadequate.

Here, we report ^{14}C results obtained from ipê leaves sampled in RJ state and its major metropolitan area (RJMA), which includes Rio de Janeiro city, during May/June of 2014. We also obtained $\delta^{13}C$ values from the same plant material. Once reproducibility between duplicates was confirmed, we revisited some of the previous sites and ran a full sampling campaign during the growing season of 2015. In 2016, we verified unexpected results and completed sampling gaps where it was feasible. The $\Delta^{14}C$ reduction over background levels (cleaner air) was then used to infer the amounts of Cff enhancement across the RJ state for 2015. While the results based on the $\delta^{13}C$ values were inconclusive, the $\Delta^{14}C$ values seem to reflect localized spikes in fossil fuel usage in certain areas within the state. This dataset offers an independent verification of GHG emissions, in particular Cff, likely associated with the city's energy and transportation sector layout during 2015. These results are discussed and compared with some of the data inventories contained in Brazilian governmental reports. To help decision making by local communities and stakeholders, we have added here a short list of recommendations to cut back on Cff emissions.

2. Materials and methods

2.1. Demographics and physical description of the area studied

Although RJ state is the fourth smallest among the 27 Brazilian states, it is the third-most populous, with 16,461,173 inhabitants [27]. Thus, with 376 people/km^2, this state has the second-largest population density after the Brazilian Federal district (Brasilia). The Rio de Janeiro state contains 91 municipalities. Those municipalities are arranged in 8 regions, including Rio de Janeiro city (the state's capital, which bears the same name as its state; Fig. 1). The RJMA encompasses Rio de Janeiro and 21 highly populated surrounding municipalities, as listed in Table 1.

The RJ state is part of the Mata Atlântica biome (reduced to <13% of its original cover [29]). It has a tropical and subtropical climate with warm or hot/humid weather, sunny days for most of the year, and average maximum and minimum temperatures of around 32 °C in summer and 18 °C in winter, respectively. Precipitation (between 1000 and 1500 mm of rain annually) tends to be concentrated during the austral summer months. The RJ state's terrain has basically three distinct features: several mountain chains (mainly in the center-southwest of the state), an eastern coastal plain facing the Atlantic Ocean, and the western plateau of the interior (Fig. 2). The mountain chains that form the physical borders between Rio de Janeiro, São Paulo, and Minas Gerais states range from 1200 to 2800 m in height, while the peaks known as Pico da Tijuca, Pedra Branca, and Gericinó are close to 1000 m in height and are located within the RJMA (Fig. 2). Rio de Janeiro city is at sea level and has 86 km of coastline to the south, and also several bays, including Guanabara Bay to the east and Sepetiba Bay to the west. The cities of Niterói and São Gonçalo are also part of the RJMA and are located across the Guanabara Bay facing the city of Rio de Janeiro. These cities are connected by a bridge (built in 1974) that is 13.29 km in length and handles approximately 150 thousand vehicles daily.

2.2. A brief history of Rio de Janeiro city development

Rio de Janeiro enjoyed a privileged position as Brazil's capital from the 18th century until 1960, boosting its geoeconomic growth. Once Rio de Janeiro lost its capital status, the city and its surrounding regions started

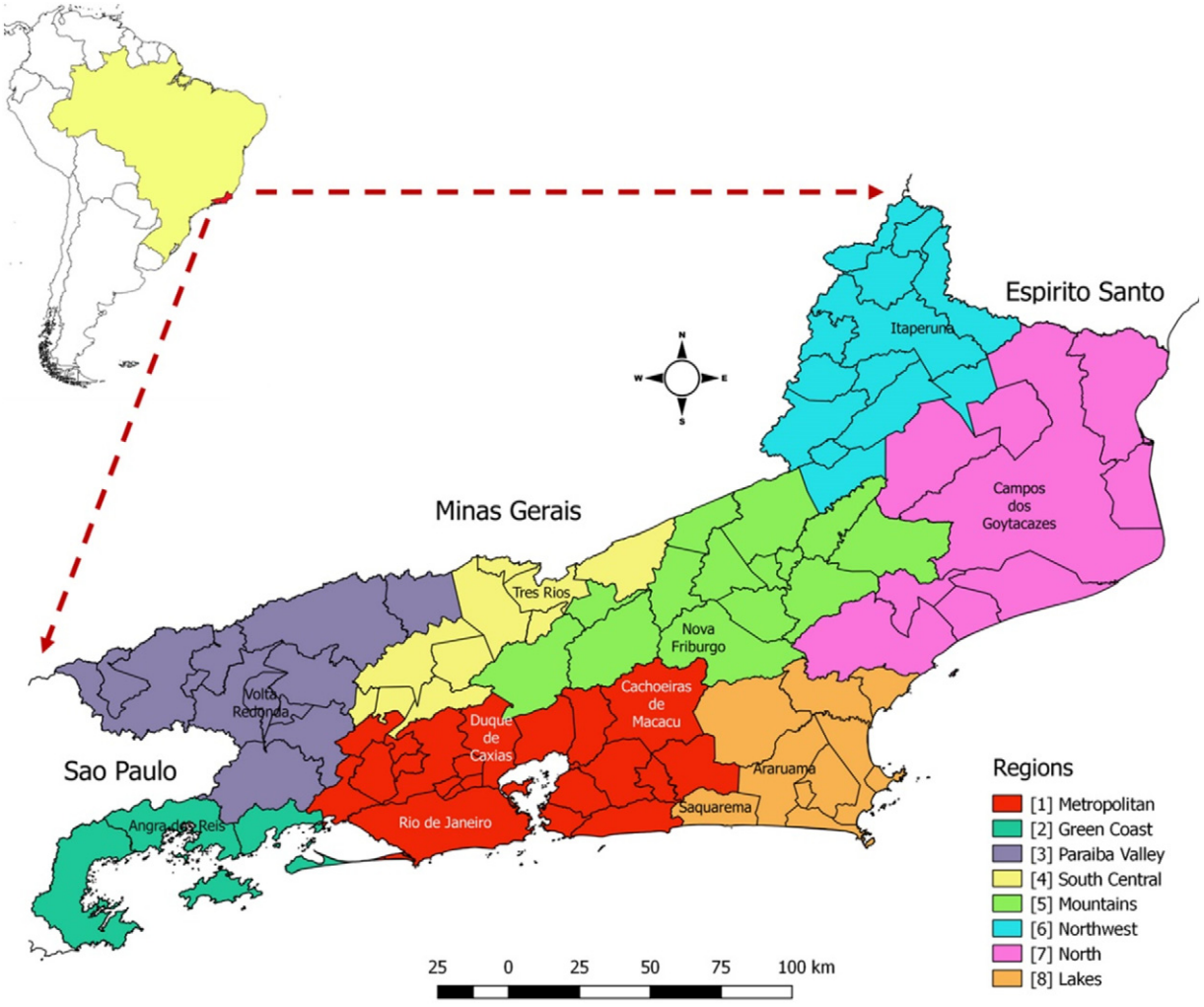

Fig. 1. Map of the Rio de Janeiro state and its 8 regions, as described in Table 1. Rio de Janeiro city is located within the metropolitan region, as indicated.

confronting significant socioeconomic and environmental problems. Massive domestic migration from Brazil's poorest rural areas, rapid urbanization, insufficient transportation, lack of public services such as urbanization, health, and sanitation, social inequality, and economic decline defined the city's demographics [30]. Districts close to the city center deteriorated and became overcrowded, while the next rings of districts, and especially those close to the coastline, were occupied by more prosperous inhabitants. Several neighborhoods further inland were then designated to accommodate the growing population in the 1960s and 1990s. Since the city grew over difficult terrain with mountains, ravines, and valleys, poor planning and population density hotspots soon created slums (informal settlements and shantytowns) pushed high into the hills and undesirable lowlands within RJMA (as identified in red in Fig. 1 and described in Table 1) and its surrounding cities [31,32]. For many years the slums lacked basic services like clean water, waste management, electricity, and paved roads. The surge of petrochemical and metallurgical industries beginning in 2001, as well as port and logistics services, resulted in an increase in the state gross domestic product (GDP), and allowed RJMA to maintain its status as the second-largest manufacturing center in the country, after São Paulo [33,34]. The areas of finance, communications, education, and entertainment also provide employment to the city's inhabitants [35]. Population density in the RJMA still follows its physical layout and the poor development growth from the 1960s. Since then the slums have extended beyond the hill slopes, toward already-overpopulated residential areas, and forced the wealthiest neighborhoods to move from the city's southern zone further west along the coast, facing the Atlantic Ocean. The city's physical expansion called for a series of highways and tunnels to be cut through its several hills. Nowadays, the western coastal zone of Rio de Janeiro is considered an upper-class neighborhood, designed to follow sustainable standards (bike paths, buses, and a subway line) to accommodate its fast-growing population. Despite the city's overall myriad of continuous problems, such as the overspread of slums, crime, and drastic levels of air and water pollution, Rio de Janeiro city was chosen to participate in the 2014 World Cup games, and to host the 2016 Summer Olympics and Paralympics games [36].

2.3. Sample selection and handling

Ipê (*Tabebuia*, from the *Bignoniaceous* family) is a deciduous perennial tree that is very popular as an ornamental tree in gardens and public spaces due to its brightly colored flowers. Ipê leaf growth occurs from late September (after the flowering period, which typically lasts 21 days) until the following May/June, when the tree is totally stripped of leaves and flowers. For this study, leaves of ipê were collected from urban and rural areas in the RJ state before the beginning of the winter (i.e., before leaf shedding). In 2014, ipê leaves were collected mostly from the smaller municipalities toward the mountain ranges (Fig. 2) to the northeast of the RJ state (e.g., Petrópolis, Itaboraí, and Cachoeiras de Macacu; Table 1), and from some urbanized spaces of Rio de Janeiro, Niterói, and São Gonçalo cities. In 2015, collection sites included most of the RJMA, Guanabara Bay surroundings, mountain ranges and hills. In 2016,

Table 1
Rio de Janeiro state regions and main municipalities.

Regions[a]	Main municipalities	Area (km^2)	Height (m)	Population[b]	Main economic features of each region
[1] Metropolitan	Rio de Janeiro	1221	0 to 1020	6,520,270	Main industries include shipyards, foundries and metallurgical plants, refineries, textiles, pharmaceutical, and food-processing. A long shoreline with multiple beaches, massifs and other physical features attracts millions of tourists yearly. Trains, buses, ferries, boats, and commercial or privately-owned vehicles connect cities and districts and take care of most of public and goods transportation. Three subway lines are found in Rio de Janeiro city (58 km in total). A 450 km-cycleway connects three beaches and some touristic sites as well. A 168-km cross-city bus rapid transit system has operated in Rio de Janeiro city since 2016.
	São Gonçalo	249	19	1,049,060	
	Duque de Caxias	465	7	887,960	
	Niterói	129	0	499,030	
	Magé	385	5	244,334	
	Itaboraí	430	17	229,630	
	Guapimirim	360	48	57,105	
	Cachoeiras de Macacu	956	54	49,340	
	Engenheiro Paulo de Frontin[a]	139	395	13,521	
[2] Green Coast	Angra dos Reis	816	0 to 1378	187,480	With the largest Atlantic forest extant, beach resorts and the historical city of Paraty, this region is famous for its tourism. It is also home to the nuclear power plants (Angra I & II) that generate about 3% of Brazil's current electricity.
	Paraty	928	5	30,580	
[3] Paraíba Valley	Volta Redonda	182	390	265,080	Known as the coffee valley region, it hosts cement factories and the second-largest Brazilian steel plant. Large equipment, aviation, and automotive manufacturers have also moved to the region.
	Resende	1094	407	119,769	
	Itatiaia	245	695	28,783	
[4] South Central	Três Rios	327	275	77,080	With the biggest road network in the country, this region contains several industries, including machinery, appliances, and metal products. Eco-tourism is also strong due to the triple-delta formation, the only one in South America.
[5] Mountains	Petrópolis	796	838	283,490	Mountain ranges, waterfalls, and a cooler climate favor tourism. Horticultural production is also strong in this region.
	Nova Friburgo	933	846	162,260	
	Teresópolis	771	871	157,200	
[6] Northwest	Itaperuna	1106	108	92,200	Once a coffee-growing empire, nowadays it is a very poor region. It has a textile and clothes manufacturing production, and a large agricultural sector, mostly devoted to milk and its byproducts. Cellulose and paper are also produced here.
	Bom Jesus do Itabapoana	598	88	30,480	
[7] North	Campos dos Goytacazes	4032	14	442,700	Deepwater oil field reservoirs can be found offshore. Major activity is agriculture, livestock, and crop production, including sugarcane for biofuel.
[8] Lakes	Maricá	362	6	150,640	Salt extraction and tourism are carried out in its 100 km coastline and freshwater marshes. A petroleum platform operates about 270 km offshore of Maricá.
	Araruama	634	15	120,490	
	Saquarema	354	2	80,840	

[a] Note that since 2017, Engenheiro Paulo de Frontin has been excluded from Region 1, but not for the period referred in this study (2014 to 2016).
[b] Population was estimated to reflect 2017, based on last census [28].

we revisited some of the previous sampling sites, and expand collection sites to some municipalities further inland.

Three to four leaves per tree were collected per location from a total of 22 sites in 2014, 75 sites in 2015, and 27 sites in 2016 (124 in total). Although several districts (zones) per municipality have been sampled more than once, just 22 distinct municipalities out of the 91 in RJ state have been visited. Among the reasons for this spatial pattern are the fact that few ipê trees were located at appropriate sites when not flowering, some locations were too difficult or dangerous to be reached for sampling, and/or some were of too low a population density to be of interest.

Upon collection, leaves were set to dry at 50–60 °C for at least 48 h or until brittle, packed in Ziploc bags, and then shipped to the W.M. Keck Carbon Cycle Accelerator Mass Spectrometry Facility at the University of California, Irvine (KCCAMS/UCI) for isotopic analysis, including radiocarbon dating by accelerator mass spectrometry (^{14}C-AMS).

2.4. Laboratory and analytical procedures

As mentioned earlier, ipê is a deciduous perennial species that, once denuded from flowers, must grow its leaves during a new season. For isotopic analysis (e.g., ^{14}C or δ^{13}C), only the lateral sections of the leaf blades were sampled at the laboratory. We assumed that the blade sections' molecular signatures are likely to be more similar than different. Furthermore, to avoid reallocated carbon from a previous season, the midrib and lateral veins were rejected as they were most likely part of the early leaflets. We then checked for isotopic agreements in single leaves by conducting isotopic measurements of material sampled from the opposing sides of the leaf midrib (indicated by letters A or B; Table S1, Appendix). We also tested discrepancies among varieties by measuring duplicate leaves of trees that flower in white, lavender-pink, and golden yellow found at the same site (indicated by numbers 1 and 2 in Table S1). Isotopic accuracy across locations was also checked by producing random duplicates for urban and non-urban areas.

Before samples were processed to determine the ^{14}C or δ^{13}C values, the leaf clippings were subjected to 2–3 consecutive baths of hot ultrapure water (>18.2 MΩ.cm) in 13 × 100 mm culture tubes for approximately 30 min to remove dust or any other superficial impurities. Once the supernatant was discarded, samples were visually inspected and set to dry at 50–60 °C in a vacuum oven system (Savant RT 100A refrigerated vapor vacuum pump) for about 1 h.

To produce CO_2, 2–3 mg of clean leaf fragments were combusted at 900 °C for 3 h following established protocols [37]. Once the CO_2 was cryogenically separated from other gases, it was then transferred

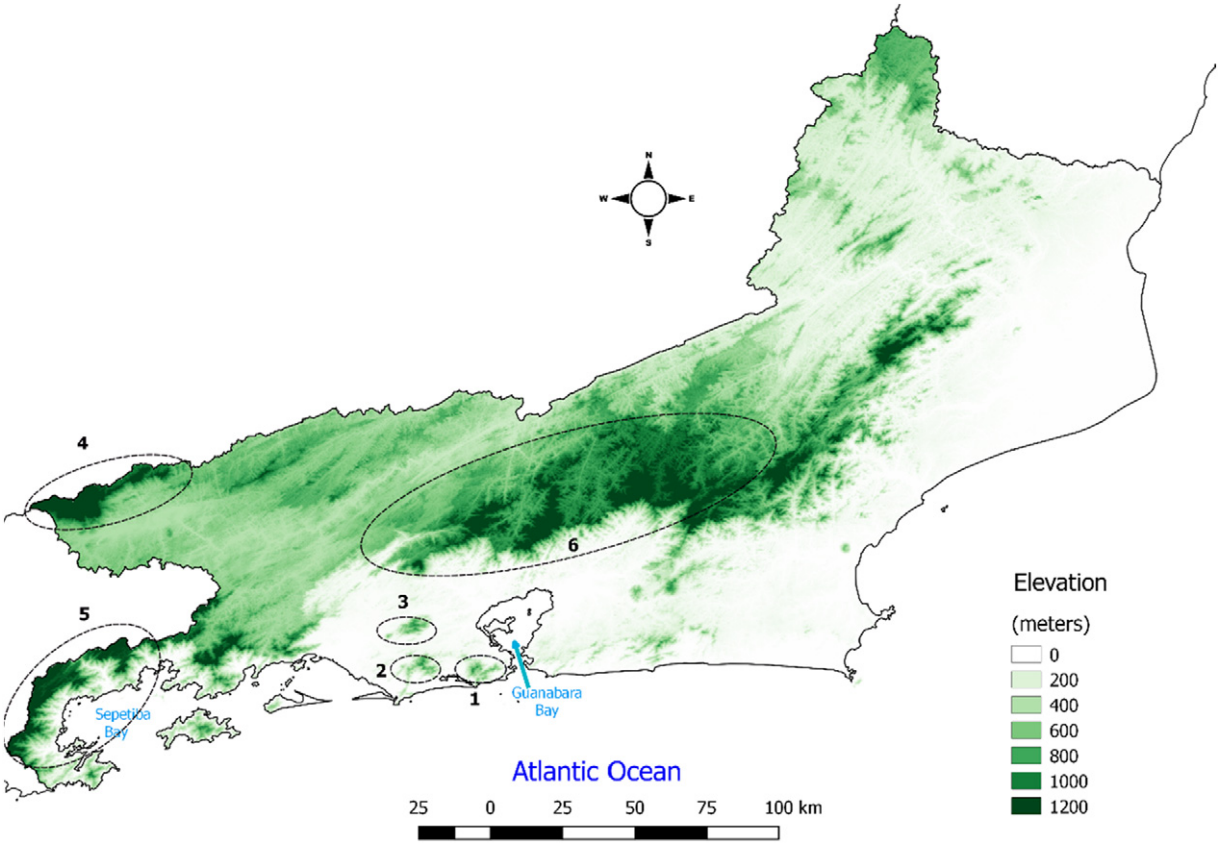

Fig. 2. Rio de Janeiro state map landform. Colored scale indicates terrain elevation. Numbers in parenthesis indicate the main massifs of Tijuca (1), Pedra Branca (2), and Gericinó (3), and the mountain ranges of Itatiaia (4), Bocaina (5) and Serra do Mar (6). The latter is a 1500 km long system of mountain ranges. Guanabara and Sepetiba bays are also indicated.

to graphitization reactors to be reduced to filamentous graphite [38]. The graphite was then pressed into aluminum target holders in preparation for ^{14}C-AMS measurements. The ^{14}C measurements were performed using an in-house modified 500 kV compact AMS unit from National Electrostatics Corporation (NEC 0.5MV 1.5SDH-21 spectrometer). Precision and accuracy in measurements are typically <3‰ [39]. The spectrometer provides the isotopic ratio $^{13}C/^{12}C$, allowing for fractionation effects (either spectrometer-induced or arising from biochemical processes) to be corrected. Blanks (^{14}C-free wood), FIRI-D and FIRI–H wood, and near-modern reference material (IAEA-C3) were also processed and measured to provide background levels and to check measurement accuracy, as an integral part of the quality control of the measurements performed at KCCAMS/UCI [40]. Measured ^{14}C values are given using the $\Delta^{14}C$ (‰) notation [41].

A smaller aliquot of CO_2 from selected samples was isolated into vials and transferred to a Gasbench II continuous-flow stable isotope ratio mass spectrometer (Delta-Plus CFIRMS) for $\delta^{13}C$ isotopic analysis. Stable isotope results are reported as δ values in ‰ relative to the Vienna Pee Dee Belemnite (vPDB), with a typical precision of 0.1‰ based on reference gas cylinders (CO_2 from CH_4 and bone-dry reference materials).

3. Results and discussion

3.1. Stable carbon isotope results

Carbon stable isotope analysis ($\delta^{13}C$) can be used to demonstrate isotopic homogeneity of the material tested. Here, we tested plant material homogeneity by probing the agreement between isotopic composition from material clipped from the opposing sides of the leaf, away from leaf-midrib and lateral veins. A pooled standard deviation based on the standard deviations of 17 duplicates (letters A or B; see Table S1, Appendix) yielded a $\delta^{13}C$ uncertainty of 0.04‰ (better than the typical precision of 0.1‰ based on reference gas cylinders).

Carbon isotope composition can be also used to understand the carbon sources and fluxes, including fossil fuel releases. On average, fossil fuel burning decreases the average $\delta^{13}C$ in ambient air from -8 to -28‰. Ideally, direct $\delta^{13}C$ measurements from air-CO_2 are desirable (e.g., [42]), as these are not influenced by net carbon fluxes derived from photosynthetic pathways and fractionation effects due to stomatal conductance, water-use efficiency, and temperature. As contributions of Cff from traffic have been demonstrated through $\delta^{13}C$ signatures of the plant-tissue of C3 grasses at the vicinity of Paris, France [43], and C4 herbs at Ghent, Belgium [44], we anticipate finding similar trends in this study even though Brazilian fossil fuels contain higher blends of biofuels than other countries' (i.e., concentrations added range from 5 to 25%). Therefore, rather than just evaluating $\delta^{13}C$ values alone, we aimed to constrain carbon sources by coupling $\delta^{13}C$ and $\Delta^{14}C$ measurements.

Ipê leaves' $\delta^{13}C$ values from a subset of samples collected in 2014 in a large gradient across RJ state vary from -26.2‰ to -35.6‰. The $\Delta^{14}C$ values for the same period were spread by as much as 20‰. Both measurements were performed on duplicate samples, as explained above. While ^{14}C data are inherently noisy due to their statistical uncertainties and corrections, reproducibility between duplicates was on the order of 2.1‰ (Section 3.2.1). Reproducibility of duplicate $\delta^{13}C$ values from leaf lateral sides was even better (i.e., 0.04‰), as mentioned earlier. However, the expected depletion in foliar of the paired $\delta^{13}C$ and $\Delta^{14}C$ values was not found.

The genera *Tabebuia* is a C4 plant type with a typical $\delta^{13}C$ value of approximately -28‰. Direct measurement of stable carbon isotopes from a pristine location at Amazon (which can be affected by canopy effects) yielded $\delta^{13}C$ value of -31‰ [45]. In Brazil, Petrobras (The Brazilian Petroleum Corporation) produced 94.4% of all the oil and natural gas

obtained in the country, which are mostly from marine fields (i.e., offshore wells produce 96% of oil and 83.7% of natural gas). As expected, both fuels are highly depleted in ^{14}C (i.e., $\Delta^{14}C \cong -1000‰$), as well as $\delta^{13}C$ (i.e., values are typically lower than −28‰, especially byproducts from natural gas, which can reach $\delta^{13}C$ values up to −40.9‰; [46,47]). Bioethanol produced in Brazil is from sugarcane and has been determined to have $\delta^{13}C$ values ranging from −12.68 up to −12.28‰ [48]. Direct $\delta^{13}C$ measurements of diesel S10 and S500, yielded values of −23.7 ± 0.1‰ and −24.9 ± 0.3‰, respectively. For the most popular biodiesel blend B7 (i.e., conventional diesel with 7% biodiesel produced from soybeans), the $\delta^{13}C$ is −23.8 ± 0.1‰ [48].

Previous direct ^{14}C measurements in several blended fuels confirmed the proportional increased addition of present-day biofuel signatures into fossil fuel depleted values, but their counterpart $\delta^{13}C$ values range from −25.6 to −27.6‰ (e.g., [50,51]). Since 1976 the Brazilian government has made it mandatory to blend anhydrous ethanol with gasoline [52]. Nowadays, most Brazilian light-vehicles run on gasoline proportions of 20–25% (E20–E25 blend), or pure hydrous ethanol (E100). The diesel fuels S10 and S500, biofuel B7, or natural gas are used mostly in buses and heavy-duty vehicles.

While we expected to see a large spread of the paired $\delta^{13}C$ and $\Delta^{14}C$ values due to the frequent usage of E100 and most of the gasoline blended biofuels (E5–E25), we also anticipated seeing a small pair trend toward depleted/negative values. As already mentioned, gasoline blended with biofuels is still much depleted in ^{14}C, even with the addition of 25% of bio-ethanol (e.g., [50,51]). However, some pair results indicated a sharp isotopic mismatch of dominant sources. For instance, isotopic results from a sample collected at Tijuca Forest massif at approximately 300 m in elevation and close to the main road appear to be highly depleted in $\delta^{13}C$ value (−35.5‰; $n = 2$), but its ^{14}C signature was from the present day, possibly from clean air or pure hydrous ethanol (E100). The site is not under closed canopy. Other pairs also display similar isotopic mismatches (Table S1). Since duplicates were processed and measured separately, a laboratory artifact could not be evoked. Sampling specific locations cannot be evoked either, as samples are from a large gradient. Therefore, no further carbon stable isotope measurements from ipê leaves were made for samples collected during the 2015 campaign, or 2016. Nonetheless, we looked into other possible explanations for these $\delta^{13}C$ and $\Delta^{14}C$ pair inconsistencies in the literature.

Wang & Pataki [13] studied spatial patterns of plant isotopes (i.e., $\delta^{13}C$, $\delta^{15}N$, $\delta^{18}O$, and $\Delta^{14}C$) in the Los Angeles area. They found significant relationships between tracers and geographic, climatic, and/or pollutant variables, including distance to atmospheric NOx sources. However, $\delta^{13}C$ distribution was way more variable, which they attributed partially to temperature and pollutants distribution.

Since nitrogen fertilization is not a standard practice in parks and gardens in RJ, the influence of nitrogen uptake (a metabolic factor) directly affecting $\delta^{13}C$ values cannot be evoked. Still, 60% of NOx is emitted by the transport sector in the city of Rio de Janeiro alone (Fig. 1), reaching an estimated maximum daily average of 80 ppb in suburban regions. This value is likely to be even higher in densely urbanized districts [53]. We then speculate that airborne pollutants, especially ozone, benzene, or sulfuric acid [54], may contribute more significant impacts than we anticipated. While all leaves collected were mature upon sampling, their appearance was very distinctive, which we initially attributed to species varieties. However, air pollutants can also cause damage to plant cell membranes, inhibiting key processes required for nutrient cycling and plant growth, affecting its overall color and texture appearance [55], and ultimately affecting carbon allocation in plant tissue [56]. Previous studies on ozone air pollution effects on vegetation confirmed its direct impact to $\delta^{13}C$ values of foliar samples (e.g., [57], and references therein). Moreover, a recent study shows that air pollutants from cities, enhanced in anthropogenic NOx, can also contribute to the background levels of ozone, NOx, and NOx oxidation products of untouched forests [58], which in turn may affect vegetation isotopic values. Novak et al. [57] also showed that ozone's effects on $\delta^{13}C$ vegetation varied among species, besides other factors, and consequently further investigations are necessary to determine what type (s) of air pollutants can directly affect the $\delta^{13}C$ values of ipê leaves in RJ.

3.2. Radiocarbon results

3.2.1. Reliability analysis

All samples were measured in six wheels in total, followed by primary standards (OXI; oxalic acid I), blanks (^{14}C-free wood), and the quality-control secondary standards (such as FIRI-D, FIRI–H, and IAEA-C3) mentioned earlier. The $\Delta^{14}C$ values were calculated from the original measurement data recorded by the spectrometer after mass-dependent isotopic fractionation correction with online-$\delta^{13}C$ values (based on spectrometer $^{13}C/^{12}C$ direct values) and sample processing background through measuring blanks [41]. At KCCAMS, 6 OXI targets are typically used per wheel measured. Long-term precision and accuracy based on standard error of normalizing OXIs and ^{14}C signatures of secondary standards have been better than 3‰ [39].

To determine whether mature ipê leaves can be used to resolve changes in $\Delta^{14}CO_2$ and thereby be used to estimate regional Cff point sources, we first checked isotopic differences within single leaf termed A and B (Table S1, Appendix). The isotopic homogeneity tests were performed in the samples collected during the first year, 2014, mostly from rural areas, although few were from urban spaces. The pooled standard deviation using the standard deviations of 17 pairs [59] produced from single leaves (by measuring the ^{14}C of material sampled from the opposing sides of the leaf midrib) was 1.7‰, indicating a good level of internal isotopic consistency. Other tests were performed in pairs of samples belonging to distinctive species varieties, growing side by side at similar geographic coordinates in Cachoeiras de Macacu (e.g., UCIAMS-143602, -144351, -143604, and -144353, measured in two wheels; Table S1). Their ^{14}C standard deviation yielded 2.1‰ ($n = 4$).

Based on the analyses reported above, the sampling campaigns during 2015 and 2016 were carried out across the entire RJ state, and ^{14}C analyses were conducted following the methods described above. Still, random duplicates of mature ipê leaves collected from the same tree (distinctive leaves) or nearby trees (with indistinctive geographic coordinates) were also measured for ^{14}C. The results from these measurements are indicated by the (1)s and (2)s in Table S1, Appendix. Although some results between leaf pairs differ significantly for no apparent reason(s), a pooled standard deviation based on the standard deviations of 33 duplicates yielded 2.1‰. We use this value to represent the total uncertainty characterized in this study, which is still lower in magnitude than some rare individual uncertainties (5 among 158 in total).

3.2.2. Regional-scale $\Delta^{14}C$ map and fossil fuel estimates

To estimate local decreases in ^{14}C signatures solely from combustion of fossil fuels input in the studied area, we obtained $\Delta^{14}C$ values (as defined in [41]) of ipê leaves in RJ state and the RJMA. The $\Delta^{14}C$ values used are shown in Table S1 (Appendix) and are for the years of 2014, 2015, and 2016. Although some of the sampling sites visited during these 3 years overlapped, they were not all identical, as the sampling campaign was concentrated in 2015. Therefore, to compose a RJ regional $\Delta^{14}C$ snapshot for 2015 and estimate its Cff contributions, we must compile all $\Delta^{14}C$ values into a single year. To fulfill this goal, we first had to eliminate the multi-year global variations by normalizing the $\Delta^{14}C$ values measured for a given reference year. We chose 2015 as the reference calendar year for the reconstruction of the RJ regional $\Delta^{14}C$ map for two main reasons: 1) its larger number of distinct sites sampled (75, versus 22 in 2014, and 27 in 2016), and 2) the actual area sampled was mostly urban-like within RJMA or close to it. The second point is quite relevant, as the contribution of CO_2 fluxes in urban areas can be highly variable on a yearly basis, while in rural areas Cff seems to be more stable and therefore follows global $^{14}CO_2$ declines closely.

To compare the data from across the three years, we first determined the most recent average annual decay displayed in the Southern Hemisphere

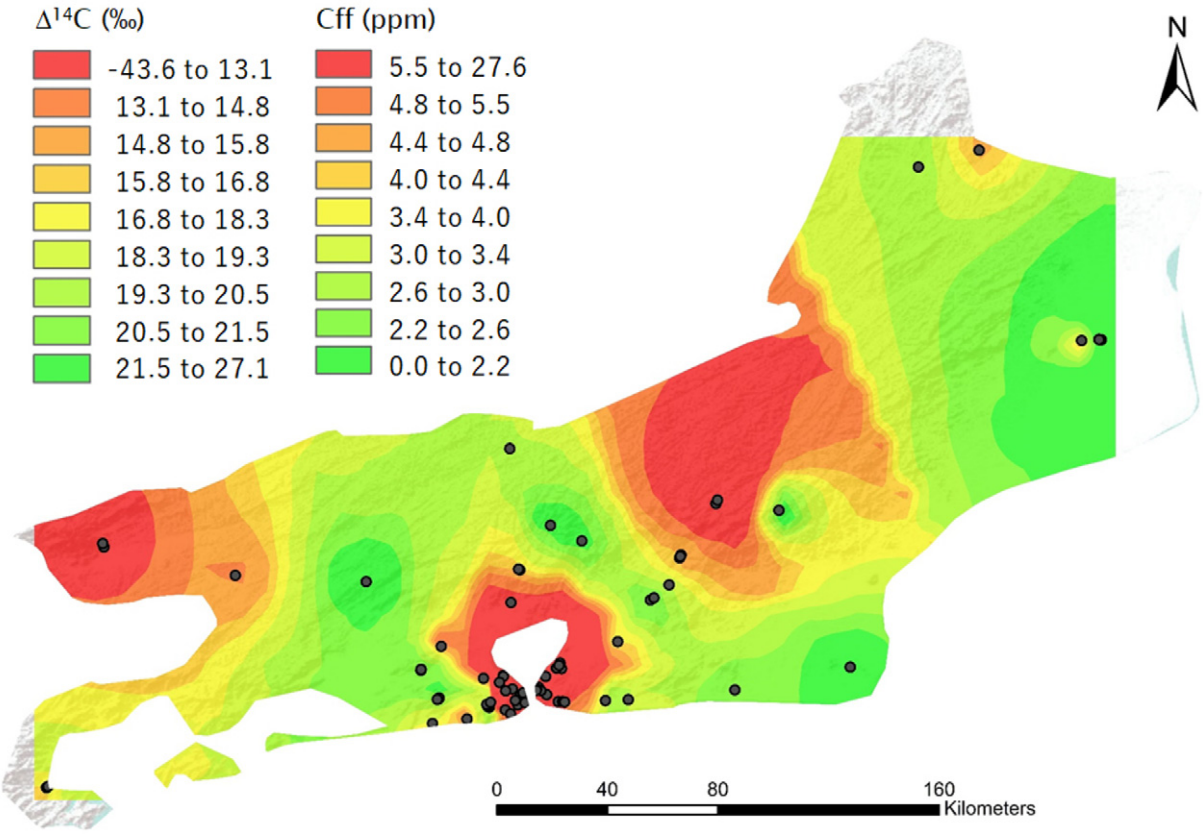

Fig. 3. The $\Delta^{14}C$ (‰) of ipê leaves in RJ (data points) corresponding to the calendar year 2015 (124 sites, 158 measurements in total). Data was mapped using Geostatistical Analyst tools in ESRI's ArcMap software. An IDW (Inverse Distance Weighted) tool was used as a method of interpolation. Local atmospheric Cff excess emissions (ppm) (legend) were derived from measured $\Delta^{14}C$ values (Table S1) and using a $\Delta^{14}C$ value of 27.1‰ ($n = 2$; average of UCIAMS-143620 & -144369 adjusted to reflect 2015) as the background level (clean-air). The estimated background concentration of CO_2 observed at a station for 2015 was obtained from NOAA as 400.36 ppm. Using similar assumptions as others [15,22,61–63] – i.e., that biospheric isotopic contributions would be similar to those of the background ($\Delta^{14}C_{bio} \approx \Delta^{14}C_{bg}$) – 1 ppm of Cff ($\Delta^{14}C = -1000$‰) would then deplete $\Delta^{14}C$ by approximately ~2.5‰. A side note with the formulae breakdown and parameter assumptions were added to the Appendix. Our ipê leaves' $\Delta^{14}C$ measurements and procedural uncertainty of 2.1‰ allow us to then infer the above-level local Cff to a precision of approximately 1 ppm. To better represent data variability, the intervals in the legend are not equal between categories.

$\Delta^{14}CO_2$ measured at Wellington, New Zealand (e.g., approximately 5‰; [60]). Since nowadays the proportion of the aboveground nuclear bomb-derived ^{14}C is essentially gone, the global average ^{14}C dilution due to the Suess effect has been decreasing steadily within a given hemisphere. This is an important condition that allows us to apply a constant correction, so that the $\Delta^{14}CO_2$ data between 2 consecutive years can be normalized (e.g., bridging 2014 into 2015, and leading 2016 back into 2015). Even if this constant correction (based on a single dataset present in [60]) is off by as much as 1‰, it will lead to a Cff uncertainty of less than ± 0.5 ppm.

Table S1 (Appendix) displays the "raw" $\Delta^{14}C$ values obtained for samples collected in all years, as well as the normalized $\Delta^{14}C$ values, as explained above. Finally, Fig. 3 presents all results as single-year (2015) $\Delta^{14}C$ values. In the same figure we also displayed the rough estimates of the equivalent Cff (color palette). The breakdown of the conventional formulation used to calculate Cff layout by others ([15,22,61–64]) appears in the Appendix.

Next, we identify the elements that must be considered when building a $\Delta^{14}C$ map and calculating fossil fuel estimates. In Fig. 4 we mapped the main features associated with energy sources and landscape cover and usage across the RJ state. This map helps to determine the optimal features influencing Cff, as it shows the distances of potential sources to the sampling points as well as the intricate pattern of urban coverage at a landscape scale.

3.2.3. Background selection

To obtain the rough estimates of Cff in ppm (displayed in the color palette in the legend of Fig. 3), we selected the highest $\Delta^{14}C$ value obtained in this study to serve as the ^{14}C content of the atmospheric background (UCIAMS-143620 & -144369; Table S1). Note that the city of Petrópolis (Region 5, Table 1), a municipality at a higher elevation in the RJ state and adjacent to the Serra do Mar hill range (Fig. 2), would yield a $\Delta^{14}C$ value of 27.1‰ ($n = 2$) if the average value in Table S1 is adjusted to 2015 as described above. This value is somewhat higher than that expected for the geographical division of the most recent ^{14}C atmospheric time-scale (zone SH1–2), if foliar growth occurred during January to June of 2015, when atmospheric $\Delta^{14}C$ would be approximately 22‰ on average (based on atmospheric air-CO_2 sampling; [60]). It must be noted that RJ state is located at low, rather than middle latitudes (Wellington, New Zealand site), and that $^{14}CO_2$ biomass tissue from a location closest to the studied area (Camanducaia, Minas Gerais) has already yielded slightly higher ^{14}C signatures as early as the 1970s [65]. If $^{14}CO_2$ time-series of Minas Gerais could be extrapolated to 2015, it would make our foliar mountain value plausible.

Therefore, in 2015 we collected two more pairs of leaves from sites in Petrópolis. One pair came from a different location in the center of the municipality than the previous year, and the second pair came from a district far away from it. Both pairs yielded very distinctive $\Delta^{14}C$ values. The one closer to the town center was relatively depleted in ^{14}C – e.g., $\Delta^{14}C = 12.0$‰ (UCIAMS-159927 & -159928; Table S1) – while the second pair, from the district of Itaipava, averaged $\Delta^{14}C = 23.6$‰ (UCIAMS-160023 & -160024; Table S1), in closer agreement with the clean-air estimates based on the New Zealand site dataset [60]. Other researchers have also observed 2–3‰ higher signatures in plant material than in the atmosphere for a single time period [14]. Some of the causes

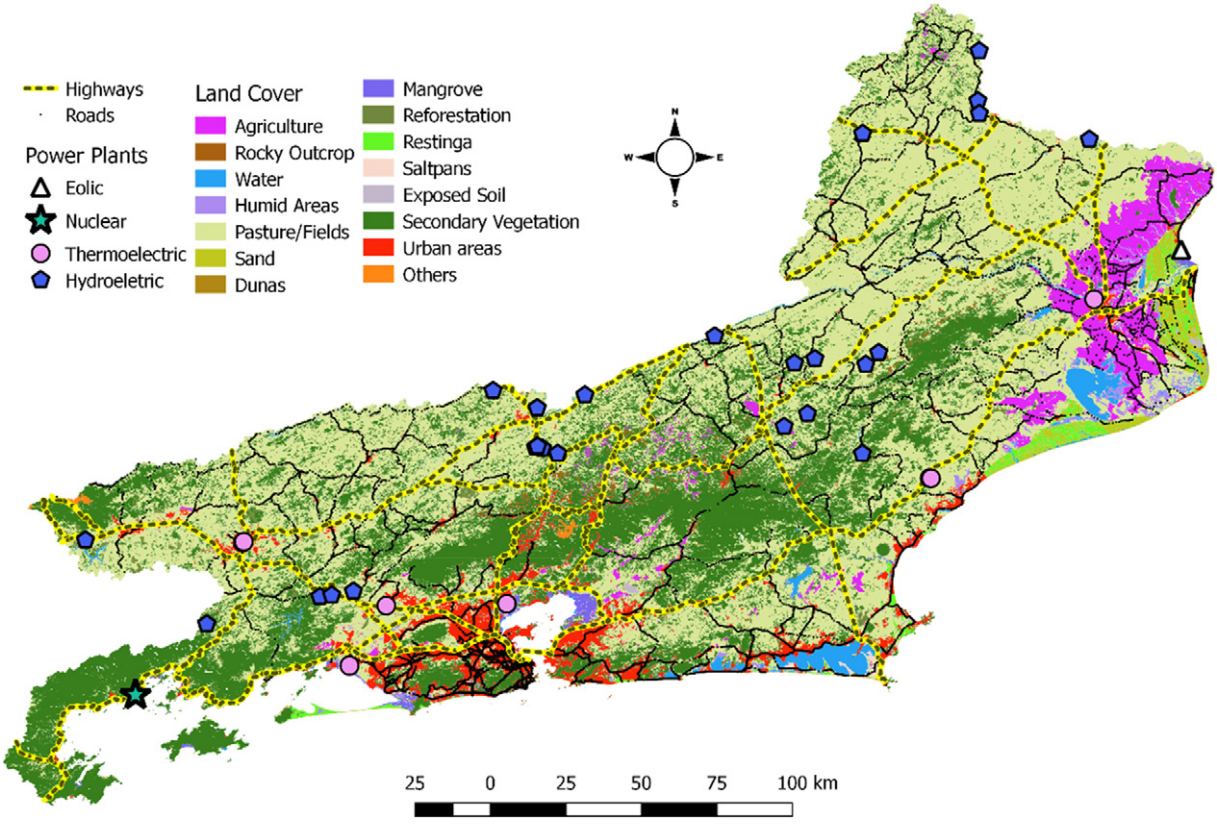

Fig. 4. Map displays RJ main energy source potentials, land cover and usage, major highways, and national roads. Due to scale constraints, just 15% of the total power plants within the state could be displayed. Those with the highest kilowatt (kW) capacity were selected in each category. For a full list of electric energy sources and production capacity visit the Brazilian Electricity Regulatory Agency (ANEEL, Agência Nacional De Energia Elétrica, http://www.aneel.gov.br/).

for the high values and offsets are clear. For instance, plant $\Delta^{14}C$ reflects the isotopic composition of diurnal atmospheric CO_2 due to the timing when photosynthesis occurs [13]. Comparisons between the same species but distinct organs or the same organs of different species tend to lead to inaccuracies, as plants build tissue and/or organs at distinct time frames. Usage of full plants and/or tissue with the possibility of reallocated carbon will be also problematic. In our study, however, besides selecting a single deciduous perennial species, we carefully sampled mature leaves before abscission, isotopic-tested clipped material away from leaf-midrib and lateral veins to avoid reallocated carbon, and checked leaves from species varieties at a single and multiple locations. These basic characteristics in sample selection and processing reduced the chances of result bias, as we demonstrated by measurements of several duplicates. Since these precautions were applied to all sites and samples, we feel that the reference background should be selected from the same plant-material dataset. Consequently, we chose to use 27.1‰ as the reference $\Delta^{14}C$ background. Furthermore, most of our study used urban data in RJ obtained during 2015, for which no adjustments to the data were required. The estimated background concentration of CO_2 for 2015 was obtained from NOAA (400.36 ppm).

3.2.4. Nuclear and biogenic contributions and biases

Since $^{14}CO_2$ can be also produced by nuclear power plants, this contribution should be taken into account in the Cff calculation. Accountability for this factor is crucial to regions that contain a high number of operational reactors (e.g., Europe [n = 182], Asia [n = 142], Northern America [n = 117]). However, the RJ state contains two operational nuclear power plants (Angra I & II) in a single complex (Fig. 4) that generates about 3% of Brazil's current electricity. Currently, those are the only operational nuclear power plants in the entire Brazilian territory. Their combined contribution to the atmosphere is at least 10 times smaller than all reactors in Europe. Kuderer et al. [66] suggested an uncertainty of about 1–2‰ in the estimated ^{14}C nuclear contamination, if the measurement site is located closer than about 30 km downwind from a nuclear facility. Their uncertainty estimate was based on $^{14}CO_2$ emissions associated with 1MWe power production (or approximately 0.5 TBq per year) for boiling-water reactor (BWR) types.

Angra I & II combined have a power production of about 2MWe. However, they are both the pressurized water reactor type (PWR), which emits ^{14}C mainly as $^{14}CH_4$. During 2005, Dias et al. [67] performed ^{14}C specific activity measurements in grass samples within an approximately 5 km perimeter zone of the nuclear complex. They concluded that the mountains behind the complex, which faces the Sepetiba Bay (Fig. 2), behave as a barrier to plume dispersion, favoring ^{14}C accumulation at the bay and its close surroundings. However, three results yielded ^{14}C values above background levels (i.e., between 1 and 18%) just outside the 5 km perimeter. Using estimates of $^{14}CO_2$ emissions from PWRs [68], the nuclear complex of Angra I & II appears to have a $^{14}CO_2$ mean emission of 0.12 TBq per year, or less. This contribution would yield a $\Delta^{14}C$ uncertainty of approximately ±0.36‰, which may or may not be detected by ^{14}C analysis if measuring sites are >30 Km downwind [66]. Our ipê leaves measurements have been at least 40 Km away from the electronuclear facilities in all directions (Fig. 3).

Regarding biogenic contributions, previous studies carried out in the Northern Hemisphere, where the seasonal cycle is strong, indicate that Cff could be consistently underestimated by 0.2 during the winter or up to 0.5 ppm during the summer ([62], and references therein). Weissert et al. [11] quantify an even higher contribution (1.0 ppm) from a residential area in subtropical Auckland, New Zealand, where the vegetation cover is dominated by evergreen vegetation (47% of surface cover fraction). RJ state is conveniently located close to the Tropic of Capricorn, where seasonal CO_2 fluctuations, due to photosynthesis and heterotrophic respiration, are attenuated compared to the Northern Hemisphere (www.esrl.noaa.gov). Regarding vegetation coverage, <8% (i.e., the forest

fragments of Itatiaia, Bocaina, and Serra do Mar, Fig. 2) of the remaining 13% of the Atlantic forest original cover exists today and crosses the RJ [29]. Furthermore, those percentages are most likely to be overestimated, as they are at least a decade old. Other vegetation surrounding the urban areas in RJ is dominated by agriculture or pasture (Fig. 4), and therefore their residence time is expected to be too low (< 1 year) to be of concern. By taking the above points into account, biogenic contributions with associated carbon of older pools across RJ state should be low or equivalent to what has been estimated for other places in the U.S. or E.U., and therefore such biases to Cff cannot possibly be higher than 0.5 ppm. Finally, the Cff uncertainty we quoted of ±1 ppm was derived from the pooled standard deviation of 33 duplicates in total (e.g., $\Delta^{14}C = 2.1‰$). This value is already greater than our typical individual measurement uncertainty (Table S1), except by two measurement results (UCIAMS-148383 & 148385). Consequently, it appears that for the RJ case the total uncertainty in Cff is so far dominated by the greater relative uncertainty of the $\Delta^{14}C$ measurements alone.

3.2.5. Spatial variability of fossil fuel CO_2 across RJ

Overall, depleted $\Delta^{14}C$ values (red gradient in Fig. 3) were concentrated around Guanabara Bay (Figs. 1 and 4) within the metropolitan area of RJMA (Region 1, Table 1), indicating high emissions of local Cff. This area encompasses the most urbanized areas of the metropolitan region, including a portion of Rio de Janeiro city composed of the districts associated with the business area (downtown) and the highly populated areas of the north zone. Depleted $\Delta^{14}C$ values were also noticeable in the busy municipalities of Duque de Caxias, and the cities of São Gonçalo and Niterói, across the Guanabara Bay (Table 1). The lowest $\Delta^{14}C$ value in our study was detected in Rio de Janeiro city, in the district of Santo Cristo ($\Delta^{14}C = -43.6‰$; UCIAMS-172001, Table S1). The ipê tree in Santo Cristo was in a park surrounding Santo Cristo dos Milagres Chapel, which nowadays is confined to a large roundabout and encircled by heavy traffic connecting the city center to the highly populated districts of the northern zone. The depleted $\Delta^{14}C$ results found here are consistent with the observations of others, in that Cff emissions are typically high and generally correlated with population density and distance to major roads, where traffic is usually heavy [13,22]. High $\Delta^{14}C$ values (closer to those of clean air) were also found within the metropolitan region (Fig. 1), mostly in association with protected greener areas and forests on higher hills, such as those shown in Figs. 2 and 5. Some wealthier residential areas along the coastline in the western zone of Rio de Janeiro city, toward Sepetiba Bay (Fig. 1), also appear to have lower Cff contributions.

Two other sites/districts in the RJ state, but outside the RJMA, showed depleted $\Delta^{14}C$ values in association with higher local Cff enhancement comparable to those of some of the busiest districts within RJMA. Those are districts in the municipalities of Nova Friburgo in the Mountain region, and Itatiaia in the Paraíba Valley region. At Nova Friburgo, the first sample was taken in 2015 near a highway, where traffic is intense and some fossil fuel emissions from heavy-duty trucks would be expected (UCIAMS-165984 & -172009; Table S1). In 2016, the same tree was revisited (UCIAMS-171989) as well as another site at the district of Vila Amélia approximately 1.4 km away from the highway (UCIAMS-171987). The latter site was less polluted than the town center, by about 50% or more. Nevertheless, the result is still significantly depleted for a region that in principle bears a lower population density than RJMA and is at a higher elevation (Table 1). Cement factories near the collection site might have contributed to the depleted result, as direct heating of limestone or burning of fossil fuels in heat kilns can produce depleted $^{14}CO_2$. The large and uneven red gradient beyond the municipality of Nova Friburgo toward the municipalities in the mountain chain, neighboring the Minas Gerais state (Fig. 3), is clearly a consequence of the sparse number of direct measurements in this area (Region 5, Table 1). The best IDW results are normally expected from simulations with sufficient sampling. However, most of the municipalities in this area, not named on maps (Figs. 1 & 2), have a low population density (<25 ka inhabitants), and were not checked. A similar effect, but less intense, was observed in the Green Coast (Fig. 3). No sampling was performed in the Bocaina mountain chains (behind the nuclear power complex, Fig. 4) or on the islands

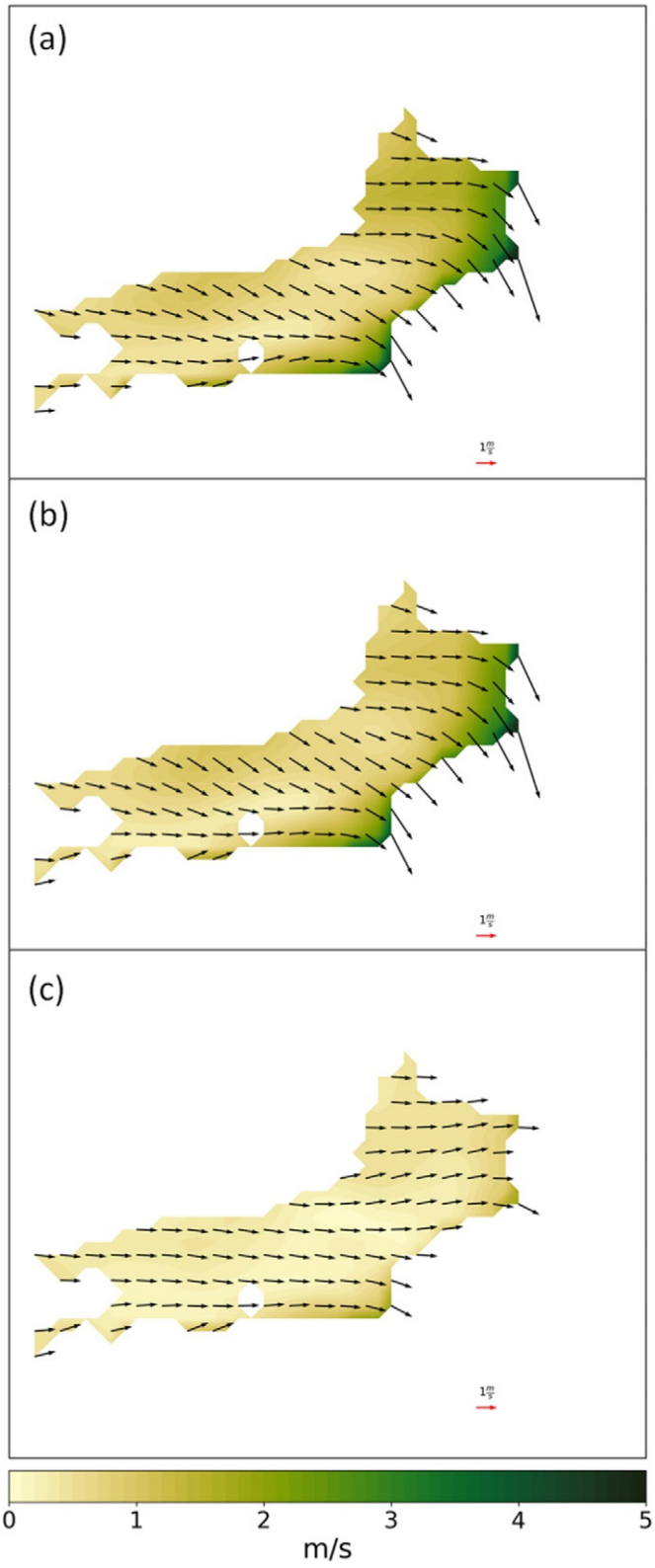

Fig. 5. Image shows the predominant wind speed and direction representative for the Rio de Janeiro state that could influence ipê leaf growth during, e.g., a) spring, b) summer, and c) fall. Wind speed intensity is shown in a palette of colors. This image was produced using monthly synoptic means of the ERA5 reanalysis wind at 10 m dataset for the period 2014 to 2016 (spatial resolution is equal 0.25°).

within the Sepetiba Bay (Region 2, Table 1 and Fig. 2) due to logistic constraints. The historical city of Paraty was instead chosen to represent this region.

At Itatiaia in Region 3 (Table 1), the ^{14}C lower values in the Africa (I) district ($\Delta^{14}C$ = 14.2‰; UCIAMS-172007, Table S1) and Centro ($\Delta^{14}C$ = 7.3‰; UCIAMS-172008, Table S1) were somewhat unexpected. Itatiaia is famous for its National Park founded in 1937, the oldest in the Brazilian territory. Its population is 10 times smaller than its neighbor, the city of Volta Redonda, which also yielded lower ^{14}C results (see UCIAMS-160016 & -160017, Table S1). This region is home to large construction equipment manufacturers and automaker plants. Metallic iron production from ore also takes place here. Sources of thermal energy in the metallurgic industry are supposedly from fuelwood-charcoal [69], and therefore its combustion byproducts should not significantly contribute to Cff. The second major steelmaker complex company in Brazil (Companhia Siderúrgica Nacional, CSN) is located in the city of Volta Redonda. Its main power source is from the thermoelectric cogeneration power plant CTE-II, also located at Volta Redonda (Fig. 4), and according to ANEEL (http://www.aneel.gov.br/), it runs mostly on fossil natural gas. Our samples at Volta Redonda were collected about 1.6 km away from the CSN complex, while those from the Itatiaia site were sampled at least 40 km from it. While the CSN complex may play a role in lowering our ^{14}C values across this entire region, it does not quite explain the very low ^{14}C results from Itatiaia, which is further away from Volta Redonda. Then again, the transit of goods in and out of the Paraíba Valley region (Region 3, Table 1) can be quite intense. Thus, we postulate that the Cff emissions we found are most likely associated with the transportation sector.

Except for the sites mentioned above, most areas inland of the RJ state showed lower Cff local contributions. Major activities in these micro-regions are agriculture, livestock, and crop production, including sugarcane for biofuel (Fig. 4). This does not preclude other types of CO_2 or GHG gases that cannot be detected by ^{14}C measurements directly.

3.2.6. Wind pattern influences on Cff emissions

The RJ state $\Delta^{14}C$ values observed from all micro-regions show various degrees of Cff emissions dependency (Fig. 3). While some of those observations may be dominated by proximity to roads, fuel type, population density, and/or major sector activities (Table 1, Fig. 4), others may be also influenced by air clusters (i.e., local hotspots with entrapped gases). The detection of entrapment of atmospheric gases over urban and rural areas is complex and may differ seasonally, due to changes in wind pattern and the influence of topographic features.

The RJ state is under the influence of the persistent South Atlantic Anticyclone, and therefore, winds oriented in a northwest-southeast direction are very common in this region throughout the year (Fig. 5). During our sampling period, these winds were stronger in intensity during the spring and summer and weaker during the fall, possibly due to the intensification of the South Atlantic Anticyclone [70]. Nonetheless, the complete growth of ipê leaves from leaflike structure to leaf maturity occurs during these three seasons.

Overall, micro-regions of the RJ state appear to be affected by its topographical features. The Serra do Mar mountain range (Fig. 2) seems to create a large wind barrier between the inland micro-regions and the coastal regions (i.e., Regions 3, 4, 5, and 6 and the inland portion of Region 7 versus Regions 1 and 8, and the coastal area of 7, in Table 1). The Paraíba Valley (Region 3) may also be affected by a regional airflow barrier created by the Itatiaia mountain range to the north, the Bocaina to the south, and the beginning of the Serra do Mar mountain range to the southeast. The Green Coast (Region 2) is completely isolated between the Bocaina hills, with its pristine Atlantic forest, and Sepetiba Bay. Furthermore, the abrupt drop in altitude toward the coastline may play a role in separating the emissions among different regions (Fig. 2). Besides uplands and hills, one must consider the effects of poor wind circulation due to unnatural obstacles such as building heights, agglomeration complexes, tunnels, and highways. Regarding district centers, and especially the overpopulated RJMA (Region 1, Table 1), wind energy stations monitored by the INEA (The State Institute of the Environment, Brazil; [71]) showed that sites in highly urbanized areas present poor air quality and very low or no wind speed. The worst such case was detected in the municipality of Duque de Caxias, followed by Niteroi and Itaborai, and in the district of Engenho de Dentro (Rio de Janeiro city). Santa Cruz, an overcrowded district of Rio de Janeiro city, showed a better air quality profile and wind pattern due to its favorable location and proximity to Sepetiba Bay.

Outside RJMA, INEA possesses wind energy stations at just four other micro-regions (i.e., Paraíba Valley, Mountains, Green Coast, and Lakes, Table 1). Overall, their seasonal wind profiles are very similar to those patterns shown in Fig. 5(a,b,c), except that of the station at Volta Redonda (Region 3). This station detected nearly calm surface winds for most of summer and fall seasons (39 to 64%, respectively) [71].

The wind pattern observations described above support our elevated regional Cff levels shown in Fig. 3, since atmospheric stability usually favors weak vertical mixing of air and thus leads to higher near-surface pollutant concentrations. In addition, the wind direction and the corridor created by orographic features (such as the Bocaina and Itatiaia mountain ranges) might play a role in the lower $\Delta^{14}C$ observed in the Paraíba Valley and Mountain regions. As previously mentioned, southeastern Brazil is the most heavily industrialized region in the country, particularly the states of São Paulo, Rio de Janeiro, and Minas Gerais. The Paraíba Valley industrial complex, with a multitude of companies, spills over into the east of São Paulo state (Fig. 1). The cities of São José dos Campos and Jacareí, both located in the Paraíba Valley region of São Paulo state, are among the top 10 Brazilian cities in CO_2 emissions [72]. A recent multi-year study on wind gradients was performed in the Mantiqueira Mountain Range (in the National Park of Itatiaia) [73]. Prevailing west winds near the top of the mountains (Region 5) and calm winds in the northern RJMA (Region 1) were found, adding evidence that terrain is a strong determining factor for air flow from local to regional scales in the RJ state, supporting the findings in this study, particularly when considered in association with neighboring CO_2 hotspots.

Wind direction and topographic barriers might have also influenced atmospheric advection of Cff into the RJ Mountains (Region 5 in Table 1). The southeast of Minas Gerais state is also known to be highly industrialized, especially the city of Juiz de Fora. This city is located at approximately 40 km from the RJ state border and contain more than a half million people and an estimated fleet of >220,000 vehicles. De Souza Araujo et al. [74] estimated that 594,048 tons of CO_2 are emitted yearly from this region. Sampling at the Minas Gerais and RJ border would be necessary to further investigate this hypothesis.

4. Fuel usage, energy consumption, and comparisons with government bottom-up inventories

Many anthropogenic activities (industry, electricity production, transportation, agriculture and crop fertilization, forest and waste management, business and residential heating) emit GHGs. Carbon dioxide from the burning of fossil fuels – i.e., Cff – is still the largest single source of GHGs in many urban areas. Nevertheless, the Brazilian biofuel economy is a well-developed industry whose roots go back to the National Alcohol Program, launched in 1975. In spite of its complicated history, biofuels still dominate states' economies and GHG emissions [75].

Brazil has a unique array of biofuel mixtures and also mandates that all light vehicles run on pure hydrous ethanol (E100), and/or gasoline blended with ethanol proportions between 20 and 25% (E20-E25 blend) [52]. Other fuels have a lesser blended mix (e.g., biodiesel is B7), or are extracted together with oil from petroleum wells (e.g., natural gas). Those are split among heavy-duty trucks, regular or BRT-type buses (within Rio de Janeiro city only), boats, ferries, and/or light-duty vehicles (such as commercial or privately-owned cars and motorcycles). Furthermore, the development of multifuel cars (over 50% of total fleet) running on either blended gasoline

Table 2
The RJ state total CO_2 emissions displayed by sectors and their associated activities during the calendar year 2015. Total CO_2 emissions include renewable sources: i.e., Cff counterpart contributors and CO_2 equivalent emissions calculated from methane (CH_4) based on ruminant animals, such as cattle, sheep, and goats (enteric fermentation). Data based on the information are accessible through SEEG (http://plataforma.seeg.eco.br/).

Sectors	Percentages (%)	Activities	Percentages (%)
Energy	69	Fuel production	37.3
		Transportation (light and heavy-duty)	27.6
		Electricity production (public service)	24.8
		Industry (include chemical reactions)	6.5
		Residential	3.1
		Business	0.5
		Public	0.2
		Farming	0.1
Residue	12	Urban waste - liquids	77
		Urban waste - solids	22.8
		Incineration	0.2
Industry	9	Metal manufacture	80.8
		Mineral products (aggregates, cement, mortar, etc.)	19.1
		Chemical industry	0.1
Agriculture	6	Enteric fermentation	72.9
		Soil management and fertilization	21.4
		Waste management, including manure	4.5
		Waste burning	1.2
Land	4	Soil alteration	93.8
		Forest residues	6.2

or pure ethanol, provides great flexibility to consumers. Natural gas was introduced to the transportation system in the late 1990s, particularly as a cheaper alternative fuel for buses. Over time, this fuel migrated from the public transportation sector to some light-duty vehicle owners in RJ state. While little is known of the full environmental impact of biofuel use, as volatile organic compounds (VOCs) studies in Brazil's southeastern region have just started [76,77], their usage is expected to greatly boost an overall reduction in GHG and some pollutant (mainly CO) emissions.

Fossil and biofuel consumption in RJ are obviously not limited to vehicular transport (Table 2). Electricity production is quite demanding in Brazil's southern region. Consequently, RJ state also requires an extensive number of power plants (Fig. 4). Many of those can use renewable sources (i.e., hydroelectric, wind, or solar) or burn biogas (from sugarcane bagasse or anaerobic digestion of biomass). Nonetheless, RJ electrical power plants still rely mostly on fossil fuel (natural gas or diesel, http://www.aneel.gov.br/). Their percentage distribution by fuel is: fossil (~70%), hydroelectric (~25%), biomass (~2%), solar (~2%), and nuclear (~1%).

RJ state air quality is also monitored by INEA for the following gases and compounds: NOx, CO, SO_2, O_3, CH, and VOCs. Unfortunately, their monitoring is quite limited across the state. A handful of stations appear to operate permanently [25,26], while others are just mobile units (INEA). Unlike the compounds mentioned above, CO_2 is not considered a classic air pollutant. Consequently, RJ CO_2 contributions must be quantified following human activities as a computing factor according to recommendations defined by the Intergovernmental Panel on Climate Change [78–80]. For RJ state, data inventories provided in Brazilian governmental reports (MCTI, Ministry of Science, Technology and Innovation, for example), research and sectoral entities, and nongovernmental organizations are normally used. The method requires tracing distinct sectors' production processes and services, and the consumption of products within political and administrative boundaries. Results computed in this way require considerable care in interpretation, as they assume minimum or no demographic crossings between regions, and some level of parameter stability for periods of time. At SEEG-Brazil (The Greenhouse Gas Emissions and Removals Estimates, http://seeg.eco.br), GHG emissions are estimated by sectors and major activities for each state.

In 2015, the RJ state reached the 10th position rank in the Brazilian territory in CO_2 emissions, with the profile shown in Table 2. On the other hand, the GHG emissions reported by the Center for Integrated Studies on Climate Change and Environment [81] gave a slightly different configuration, arranging agriculture and land use sectors together and breaking down emissions by micro-regions. Again, the energy sector dominated the emissions in the state. Cumulative energy sector emissions by micro-region were broken down as follows: North (48.4%), Metropolitan (34.0%), Paraíba Valley (10.4%), Lakes (2.4%), Mountains (2.3%), South Central (1.0%), Northwest (0.9%), and Green Coast (0.6%). Emissions were then further evaluated as energy consumption. In this case the Metropolitan region was placed first, followed by the North and Paraíba Valley. Lakes and Mountains regions had far less CO_2 emissions in this sector. Still, in all cases the transport subsector (in particular, fuel usage) accounted for the largest CO_2 atmospheric contributions in 2015, except in the north, where agriculture, thermoelectric power, and natural gas production activities dominated. This assessment is in agreement with our findings (Fig. 3), as we did not assign a significant local Cff contribution at the north RJ sub-region (GHG emissions by livestock and agriculture management are expected to dominate in this area).

5. Considerations for future studies and public policies

The results obtained in this study could be used in conjunction with other studies to further improve the mitigation plans in RJ state. Energy is the main factor for CO_2 emissions in the state, corresponding to about two-thirds of total CO_2 emissions, and, from these, fuel production, transportation, and electricity production correspond to the largest portions (Table 2). A comprehensive prognostic evaluation of energy demand for the RJ state, accounting for national and local economic growth, technology improvements, etc., should be performed to better locate the main issues to be dealt with in the future: e.g., which sectors will be more or less important, which regions will experience the highest economic growth. Regarding Cff alone, a few considerations can be made concerning mitigations in RJ and RJMA:

- Concerning the RJMA state, where the transport sector is very relevant, a few actions could be implemented to help mitigate Cff hotspots, for example, upgrading or improving urban mobility. Improving public transport with focus on hybrid electric/biofuel technology could certainly lead to important gains in this sector, especially around the Guanabara Bay (Fig. 1). While RJ city had already improved Cff levels at the western coastal zone by creating alternative public transportation during 2015 and 2016 (Table 1), other municipalities surrounding the bay must deal with the yearly vehicular increase of almost 100,000 units. Public policies aimed toward better environmental and social justice are paramount to achieving these goals, particularly when coupled with local community engagement. Also, some studies have shown the importance of ship emissions in coastal cities ([82], and references therein), which brings another challenge when managing Cff levels in the RJMA bays. In the long term, decentralizing economic activities and generating better job opportunities in the most populated but peripheral districts could help bring home and employment closer, decreasing the growing use of private cars and traffic congestion, the need for commuting, and thereby, transport emissions.
- Decentralizing energy production and boosting local renewable energy use could help immensely to reduce Cff usage. For that purpose, maps with the state's potential renewable energy – solar, wind, tidal, hydroelectric, etc. – could be used to better guide renewable energy investments, and as a way to best use the local potentialities [83]. Moreover, fossil fuel (natural gas/diesel) is still largely used in RJ thermoelectric power plants, as well as in similar units in the neighboring states of São Paulo and Minas Gerais (Fig. 1). However, those states have also implemented more renewable types of power plants (i.e., biogas type) in their territories than RJ (http://www.aneel.gov.br/). The methodology

we present here, using samples of ipê leaves and ^{14}C measurements, represents a relatively cheap and efficient way for monitoring the sustainable transition from fossil to renewable energy in any chosen location of the state.

- Worrisome are the high Cff hotspots with less anthropogenic activity in RJ state (e.g., Petrópolis and Itatiaia, Fig. 3 and Section 3.2.5), which demonstrate the relevance of the regional Cff contributions from neighboring states (i.e., São Paulo and Minas Gerais). This problem demonstrates the importance of regional and state-level environmental governance. Regional plans and actions must be developed and implemented conjointly with these neighboring states in order to reach a mitigation level appropriate for the whole of the southeast Brazilian region, the most important economic and industrial region in the South American continent.

6. Summary

Here, we demonstrated that ^{14}C measurements of mature ipê leaves can be used to detect an excess of atmospheric Cff. Depleted $^{14}CO_2$ was observed, expressed as $\Delta^{14}C$, in association with Cff enhancements closer to sources (such as roads) and/or areas with large population densities and industrial complexes. The RJ state's topographical features, with several mountain ranges, massifs, valleys, and depressions, coupled with its wind patterns, seem to impact Cff by dividing the state into inland and coastal emitters. Areas with higher Cff levels were found in districts in the Paraíba Valley (Region 3) and Mountain (Region 5) as well as areas surrounding Guanabara Bay in the RJMA (Region 1), where population density and traffic volumes are higher. Significantly lower Cff contributions were observed in the Northwest (Region 6) and Lakes (Region 8), which are dominated by agriculture and tourism activities. Our findings support previous interpretations that daily traffic and industrial emissions still have a significant impact on the RJ state Cff levels. Also, CO_2 fluxes from neighboring regions of São Paulo and Minas Gerais states (São Paulo Paraíba Valley and Juiz de Fora, respectively), coupled with distinctive regional air flow pathways, may be responsible for the low $\Delta^{14}C$ values (i.e., high Cff) found in the RJ Paraíba Valley and the Mountain regions.

The 2006 IPCC guidelines recommended identifying GHG emissions from the production and consumption of goods occurring within a political and administrative boundary. Atmospheric CO_2 loading due to fossil fuel combustion alone is still a major global concern. Estimates of RJ state GHG emissions, including fossil fuel CO_2, are currently based on economic statistics, where flex-fuel vehicles and fuel types dictate emission source trends. In RJ state the energy sector and fuel consumption seem to dominate CO_2 emissions, but local patterns are still very unclear.

Our dataset, based on regional fossil fuel CO_2 distribution through $\Delta^{14}C$ values of ipê leaves, provides a basis for developing air pollution legislation and for establishing more sophisticated monitoring approaches, including placement of future monitoring stations across the RJ state. Until higher-frequency, atmosphere-based air-CO_2 determinations or continuous measurements of trace gas concentrations (including CO_2 and CO) to enable a near "real-time" monitoring of fossil fuel emissions cannot be fully implemented, an independent assessment of bottom-up Cff based on careful plant tissue ^{14}C measurements (such this study) can help to determine whether non-renewable fuel emission reduction actions are achieving their goals, and/or data assembled via statistical reports can be corroborated. In summary, $\Delta^{14}C$ distribution maps from ipê leaves and this analysis provide a fast and effective approach for tracing local Cff contributions.

Acknowledgments

Funding for all isotopic data was provided by the Keck Carbon Cycle Accelerator Mass Spectrometry Laboratory at UCI through GMS. We also thank the Brazilian funding agencies CNPq (Conselho Nacional de Desenvolvimento Científico e Tecnológico), CAPES (Coordenação de Aperfeiçoamento de Pessoal de Nível Superior), FAPERJ (Fundação de Amparo à Pesquisa do Estado do Rio de Janeiro), and PRONEX (Programa de Apoio a Núcleos de Excelência) for student support. Sample collection was made possible through the assistance of several colleagues and family members of the co-authors. Special thanks are given to Eduardo Queiroz, Josemar Costa, Marcelo Muniz, Renan Cardoso, and Glaziele Campbell for helping with the sampling. GMS wishes to thank Jocelyn Turnbull for valuable advice. The authors also wish to extend their thanks to the Editor and the reviewers for their constructive comments.

Author contributions

GMS conceived the study. GMS, FO, and KM selected the species tested and designed the experiments. GMS, FO, and CSGG processed and analyzed radiocarbon samples. GMS and JP analyzed the radiocarbon data and built the ^{14}C distribution map. ACTS and JBC help on figures presentations, and interpretation of the study's findings. GMS wrote the paper with input from all authors.

Appendix A. Supplementary data

Supplementary data to this article can be found online at https://doi.org/10.1016/j.cacint.2019.06.001.

References

[1] IPCC, 2015. Intergovernmental Panel on Climate Change, 2015. Climate change 2014: mitigation of climate change (Vol. 3). Cambridge University Press.
[2] Vogel F, Hamme S, Steinhof A, Kromer B, Levin I. Implication of weekly and diurnal 14C calibration on hourly estimates of CO-based fossil fuel CO2 at a moderately polluted site in southwestern Germany. Tellus B Chem Phys Meteorol 2010;62(5):512–20.
[3] Fischer ML, Parazoo N, Brophy K, Cui X, Jeong S, Liu J, et al. Simulating estimation of California fossil fuel and biosphere carbon dioxide exchanges combining in situ tower and satellite column observations. J Geophys Res-Atmos 2017;122:3653–71 https://doi.org/10.1002/2016JD025617.
[4] Turnbull J, Karion A, Fischer ML, Faloona I, Guilderson T, Lehman SJ, et al. Assessment of fossil fuel carbon dioxide and other anthropogenic trace gas emissions from airborne measurements over Sacramento, California in spring 2009. Atmos Chem Phys 2011;11:705–21.
[5] Turnbull JC, Keller ED, Baisden T, Brailsford G, Bromley T, Norris M, et al. Atmospheric measurement of point source fossil CO2 emissions. Atmos Chem Phys 2014;14:5001–14.
[6] Turnbull JC, Sweeney C, Karion A, Newberger T, Lehman SJ, Tans PP, et al. Towards quantification and source sector identification of fossil fuel CO2 emissions from an urban area: results from the INFLUX experiment. J Geophys Res Atmos 2014;120(1):292–312.
[7] Wu D, Lin JC, Fasoli B, Oda T, Ye X, Lauvaux T, et al. A Lagrangian approach towards extracting signals of urban CO2 emissions from satellite observations of atmospheric column CO2 (XCO2): X-Stochastic Time-Inverted Lagrangian Transport model ("X-STILT v1"). Geosci Model Dev 2018;11(12):4843.
[8] Zeng ZC, Lei L, Strong K, Jones DB, Guo L, Liu M, et al. Global land mapping of satellite-observed CO2 total columns using spatio-temporal geostatistics. Int J Digit Earth 2017;10(4):426–56.
[9] Miller JB, Lehman SJ, Montzka SA, Sweeney C, Miller BR, Karion A, Wolak C, Dlugokencky EJ, Southon J, Turnbull JC, Tans PP. Linking emissions of fossil fuel CO2 and other anthropogenic trace gases using atmospheric 14CO2. Journal of Geophysical Research: Atmospheres 2012;117(D8).
[10] Turnbull J, Guenther D, Karion A, Sweeney C, Anderson E, Andrews A, et al. An integrated flask sample collection system for greenhouse gas measurements. Atmos Meas Tech 2012;5(9):2321–7.
[11] Weissert LF, Salmond JA, Turnbull JC, Schwendenmann L. Temporal variability in the sources and fluxes of CO2 in a residential area in an evergreen subtropical city. Atmos Environ 2016;143:164–76.
[12] Garnett MH, Murray C. Processing of CO2 samples collected using zeolite molecular sieve for 14C analysis at the NERC Radiocarbon Facility (East Kilbride, UK). Radiocarbon 2013;55(2):410–5.
[13] Wang WW, Pataki DE. Spatial patterns of plant isotope tracers in the Los Angeles urban region. Landsc Ecol 2010;25:35–52.
[14] Bozhinova D, Combe M, Palstra SWL, Meijer HAJ, Krol MC, Peters W. The importance of crop growth modeling to interpret the Δ14CO2 signature of annual plants. Global Biogeochem Cycles 2013;27(3):792–803.
[15] Hsueh DY, Krakauer NY, Randerson JT, Xu X, Trumbore SE, Southon JR. Regional patterns of radiocarbon and fossil fuel-derived CO2 in surface air across North America. Geophys Res Lett 2007;34(2):6–11.
[16] Xi XT, Ding XF, Fu DP, Zhou LP, Liu KX. Δ14C level of annual plants and fossil fuel derived CO2 distribution across different regions of China. Nuclear Instruments and Methods in Physics Research Section B: Beam Interactions with Materials and Atoms 2013;294:515–9.
[17] Park JH, Hong W, Park G, Sung KS, Lee KH, Kim YE, et al. Distributions of fossil fuel originated CO2 in five metropolitan areas of Korea (Seoul, Busan, Daegu, Daejeon,

and Gwangju) according to the Δ14C in ginkgo leaves. Nucl Inst Methods Phys Res B 2013;294:508–14.
[18] Park JH, Hong W, Park G, Sung KS, Lee KH, Kim YE, et al. A comparison of distribution maps of Δ14C in 2010 and 2011 in Korea. Radiocarbon 2013;55(2):841–7.
[19] Park JH, Hong W, Xu X, Park G, Sung KS, Sung K, et al. The distribution of Δ14C in Korea from 2010 to 2013. Nucl Inst Methods Phys Res B 2015;361:609–13.
[20] Bozhinova D, Palstra SWL, van der Molen MK, Krol MC, Meijer HAJ, Peters W. Three years of Δ14CO2 observations from maize leaves in the Netherlands and Western Europe. Radiocarbon 2016;58(3):459–78.
[21] Quarta G, Rizzo GA, D'Elia M, Calcagnile L. Spatial and temporal reconstruction of the dispersion of anthropogenic fossil CO2 by 14C AMS measurements of plant material. Nucl Instrum Methods Phys Res, Sect B 2007;259(1):421–5.
[22] Riley WJ, Hsueh DY, Randerson JT, Fischer ML, Hatch JG, Pataki DE, Wang W, Goulden ML. Where do fossil fuel carbon dioxide emissions from California go? An analysis based on radiocarbon observations and an atmospheric transport model. Journal of Geophysical Research: Biogeosciences 2008;113(G4). https://doi.org/10.1029/2007JG000625.
[23] Heilig GK. World urbanization prospects: the 2011 revision. United Nations, Department of Economic and Social Affairs (DESA), Population Division. New York: Population Estimates and Projections Section; 2012; 14.
[24] Romeiro V, Parente V. Climate change regulation in Brazil and the role of subnational governments, chapter 2. In: Motta RSD, Hargrave J, Luedemann G, Gutierrez S, Pereira MBG, editors. Climate change in Brazil: economic, social and regulatory aspects. Brasília: Institute for Applied Economic Research – Ipea; 2011 [358 pp.].
[25] Martins LD, Wikuats CFH, Capucim MN, de Almeida DS, da Costa SC, Albuquerque T, et al. Extreme value analysis of air pollution data and their comparison between two large urban regions of South America. Weather Clim Extrem 2017;18:44–54.
[26] Silva CM, Corrêa SM, Arbilla G. Determination of CO2, CH4 and N2O: a case study for the city of Rio de Janeiro using a new sampling method. J Braz Chem Soc 2016;27(4):778–86.
[27] IBGE. Instituto Brasileiro de Geografia e Estatistica: Planejamento, desenvolvimento e Gestão. http://www.planejamento.gov.br/acesso-a-informacao/auditorias/instituto-brasileiro-de-geografia-e-estatistica-ibge/instituto-brasileiro-de-geografia-e-estatistica-ibge-2014; 2014.
[28] IBGE. Instituto Brasileiro de Geografia e Estatistica. https://censo2010.ibge.gov.br/apps/atlas/; 2010.
[29] Ribeiro MC, Metzger JP, Martensen AC, Ponzoni FJ, Hirota MM. The Brazilian Atlantic Forest: how much is left, and how is the remaining forest distributed? Implications for conservation. Biol Conserv 2009;142(6):1141–53.
[30] Grostein MD. Metrópole e expansão urbana: a persistência de processos "insustentáveis". São Paulo Perspect 2001;15(1):13–9.
[31] Brito F, Horta CJG, AMARAL EDL. A urbanização recente no Brasil e as aglomerações metropolitanas. XXIV IUSSP General Conference; 2001, August. p. 168–84.
[32] Fernandes VA, Henríquez C, Soto CL. A city to live or work in? Contradictions present in the spatial distribution of economic activities, transport and social conditions: a case study of the city of Rio de Janeiro. Espaço Aberto 2017;7(2):157–79.
[33] Geiger P. Mudanças no Espaço Econômico Brasileiro. IBGE, Atlas Nacional do Brasil Rio de Janeiro, RJ Grostein, M.D., 2001. Metrópole e expansão urbana: a persistência de processos "insustentáveis", vol. 15(1). São Paulo em perspectiva; 2000. p. 13–9.
[34] Stamm C, Staduto JAR, Lima JFD, Wadi YM. Urban population and dissemination of medium size cities in Brazil. Interações (Campo Grande) 2013;14(2):251–65.
[35] Iwata N, Del Rio V. The image of the waterfront in Rio de Janeiro: urbanism and social representation of reality. J Plan Educ Res 2004;24(2):171–83.
[36] Aaron Richmond M, Garmany J. 'Post-Third-World city' or neoliberal 'city of exception'? Rio de Janeiro in the Olympic Era. Int J Urban Reg Res 2016;40(3):621–39.
[37] Santos GM, Southon JR, Druffel-Rodriguez KC, Griffin S, Mazon M. Magnesium perchlorate as an alternative water trap in AMS graphite sample preparation: a report on sample preparation at KCCAMS at the University of California, Irvine. Radiocarbon 2004;46:165–73.
[38] Santos GM, Moore R, Southon J, Griffin S, Hinger E, Zhang D. AMS 14C preparation at the KCCAMS/UCI Facility: status report and performance of small samples. Radiocarbon 2007;49(2):255–69.
[39] Beverly RK, Beaumont W, Tauz T, Ormsby KM, von Reden KF, Santos GM, Southon JR. The Keck Carbon Cycle AMS Laboratory, University of California, Irvine: status report. Radiocarbon 2010;52(2–3):301–9.
[40] Santos GM, Ormsby K. Behavioral variability in ABA chemical pretreatment close to the 14C age limit. Radiocarbon 2013;55:534–44.
[41] Stuiver M, Polach HA. Discussion: reporting of 14C data. Radiocarbon 1977;19(3):355–63.
[42] Takahashi HA, Konohira E, Hiyama T, Minami M, Nakamura T, Yoshida N. Diurnal variation of CO2 concentration, Δ14C and δ13C in an urban forest: estimate of the anthropogenic and biogenic CO2 contributions. Tellus B Chem Phys Meteorol 2002;54(2):97–109.
[43] Lichtfouse E, Lichtfouse M, Jaffrézic A. δ13C values of grasses as a novel indicator of pollution by fossil-fuel-derived greenhouse gas CO2 in urban areas. Environ Sci Technol 2003;37(1):87–9.
[44] Balasooriya BLWK, Samson R, Mbikwa F, Boeckx P, Van Meirvenne M. Biomonitoring of urban habitat quality by anatomical and chemical leaf characteristics. Environ Exp Bot 2009;65(2–3):386–94.
[45] Magnusson WE, de Araújo MC, Cintra R, Lima AP, Martinelli LA, Sanaiotti TM, et al. Contributions of C3 and C4 plants to higher trophic levels in an Amazonian savanna. Oecologia 1999;119(1):91–6.
[46] Mello MR, Gaglianone PC, Brassell SC, Maxwell JR. Geochemical and biological marker assessment of depositional environments using Brazilian offshore oils. Mar Pet Geol 1988;5(3):205–23.
[47] Prinzhofer A, Rocha Mello M, Takaki T. Geochemical characterization of natural gas: a physical multivariable approach and its applications in maturity and migration estimates. AAPG Bull 2000;84(8):1152–72.
[48] Neves LA, Sarmanho GF, Cunha VS, Daroda RJ, Aranda DA, Eberlin MN, et al. The carbon isotopic (13C/12C) signature of sugarcane bioethanol: certifying the major source of renewable fuel from Brazil. Anal Methods 2015;7(11):4780–5.
[49] dos Santos VHJ, Ramos AS, Pires JP, Engelmann PDM, Lourega RV, Ketzer JM, Rodrigues LF. Discriminant analysis of biodiesel fuel blends based on combined data from Fourier Transform Infrared Spectroscopy and stable carbon isotope analysis. Chemom Intel Lab Syst 2017;161:70–8.
[50] Culp R, Cherkinsky A, Prasad GR. Comparison of radiocarbon techniques for the assessment of biobase content in fuels. Appl Radiat Isot 2014;93:106–9.
[51] Dijs IJ, Van der Windt E, Kaihola L, van der Borg K. Quantitative determination by 14C analysis of the biological component in fuels. Radiocarbon 2006;48(3):315–23.
[52] ANFAVEA (Associação Nacional dos Fabricantes de Veículos Automotores). Anuário da Indústria Automobilística Brasileira 2015/Brazilian Automotive Industry Yearbook 2015. São Paulo. Available at: www.anfavea.com.br; 2015.
[53] Rodrigues F, Milas I, Martins EM, Arbilla G, Bauerfeldt GF, Paula MD. Experimental and theorical study of the air quality in a suburban industrial-residential area in Rio de Janeiro, Brazil. J Braz Chem Soc 2007;18(2):342–51.
[54] Middleton J, Crafts A, Brewer R, Taylor O. Plant damage by air pollution: visible injury to plants by atmospheric pollutants amounts to annual loss of millions of dollars in some affected areas. Calif Agric 1956;10(6):9–12.
[55] Moura BB, Alves ES, Marabesi MA, de Souza SR, Schaub M, Vollenweider P. Ozone affects leaf physiology and causes injury to foliage of native tree species from the tropical Atlantic Forest of southern Brazil. Sci Total Environ 2018;610:912–25.
[56] Dhir B. Air pollutants and photosynthetic efficiency of plants. Plant responses to air pollution. Singapore: Springer; 2016. p. 71–84 https://doi.org/10.1007/978-981-10-1201-3_7.
[57] Novak K, Cherubini P, Saurer M, Fuhrer J, Skelly JM, Kräuchi N, et al. Ozone air pollution effects on tree-ring growth, δ13C, visible foliar injury and leaf gas exchange in three ozone-sensitive woody plant species. Tree Physiol 2007;27(7):941–9.
[58] Wei D, Fuentes JD, Gerken T, Trowbridge AM, Stoy PC, Chamecki M. Influences of nitrogen oxides and isoprene on ozone-temperature relationships in the Amazon rain forest. Atmospheric Environment 2019;206:280–92.
[59] Cohen J. Statistical power analysis for the behavioral sciences. 2nd ed. Hillsdale: Lawrence Erlbaum; 1988.
[60] Turnbull JC, Mikaloff Fletcher SE, Ansell I, Brailsford GW, Moss RC, Norris MW, et al. Sixty years of radiocarbon dioxide measurements at Wellington, New Zealand: 1954–2014. Atmos Chem Phys 2017;17:14771–84 https://doi.org/10.5194/acp-17-14771-2017.
[61] Turnbull JC, Miller JB, Lehman SJ, Tans PP, Sparks RJ, Southon J. Comparison of 14CO2, CO, and SF6 as tracers for recently added fossil fuel CO2 in the atmosphere and implications for biological CO2 exchange. Geophys Res Lett 2006;33:L01817. https://doi.org/10.1029/2005GL024213.
[62] Turnbull J, Rayner P, Miller J, Naegler T, Ciais P, Cozic A. On the use of 14CO2 as a tracer for fossil fuel CO2: quantifying uncertainties using an atmospheric transport model. J Geophys Res 2009;114(D22):302. https://doi.org/10.1029/2009JD012308.
[63] Xi XT, Ding XF, Fu DP, Zhou LP, Liu KX. Regional Δ14C patterns and fossil fuel derived CO2 distribution in the Beijing area using annual plants. Chin Sci Bull 2011;56:1721–6.
[64] Levin I, Kromer B, Schmidt M, Sartorius H. A novel approach for independent budgeting of fossil fuel CO2 over Europe by 14CO2 observations. Geophysical Research Letters 2012;30(23):2194. https://doi.org/10.1029/2003GL018477.
[65] Santos GM, Linares R, Lisi CS, Tomazello Filho M. Annual growth rings in a sample of Paraná pine (Araucaria angustifolia): toward improving the 14C calibration curve for the Southern Hemisphere. Quat Geochronol 2015;25:96–103.
[66] Kuderer M, Hammer S, Levin I. The influence of 14CO2 releases from regional nuclear facilities at the Heidelberg 14CO2 sampling site (1986–2014). Atmos Chem Phys 2018;18(11):7951–9.
[67] Dias CM, Santos RV, Stenström K, Nícoli IG, Skog G, da Silveira Corrêa R. 14C content in vegetation in the vicinities of Brazilian nuclear power reactors. J Environ Radioact 2008;99(7):1095–101.
[68] Graven HD, Gruber N. Continental-scale enrichment of atmospheric 14CO2 from the nuclear power industry: potential impact on the estimation of fossil fuel-derived CO2. Atmos Chem Phys 2011;11:12339–49 https://doi.org/10.5194/acp-11-12339-2011.
[69] Uhlig A, Goldemberg J, Coelho ST. O uso de carvão vegetal na indústria siderúrgica brasileira e o impacto sobre as mudanças climáticas. Rev Bras Energ 2008;14(2):67–85.
[70] Nobre CA, Marengo JA, Seluchi ME, Cuartas LA, Alves LM. Some characteristics and impacts of the drought and water crisis in Southeastern Brazil during 2014 and 2015. J Water Resour Prot 2016;8(02):252.
[71] INEA, 2015 - Relatório Anual de Qualidade do Ar do Estado do Rio de Janeiro 2015. Rio de Janeiro, 2015 (download - www.inea.rj.gov.br - document inea0131852.pdf).
[72] São Paulo state, 2018, ANUÁRIO DE ENERGÉTICOS POR MUNICÍPIO NO ESTADO DE SÃO PAULO - 2018 ano base 2017, Secretaria de Energia e Mineração, São Paulo, 2018; 122pp (http://www.energia.sp.gov.br/).
[73] Sobral BS, Oliveira Júnior JFD, Gois GD, Terassi PMDB, Pereira CR. Wind regime in Serra do Mar Ridge-Rio de Janeiro, Brazil. Rev Bras Meteorol 2018;33(3):441–51.
[74] De Souza Araujo C, de Almeida Nogueira I, Procópio AS. Inventário de fontes móveis emissoras de poluentes atmosféricos na cidade de Juiz de Fora-MG. Revista Eletrônica Principia 2013;17:81–9.
[75] Pinguelli L, Villela RA, de Campos CP. Biofuels in Brazil in the context of South America energy policy. Chapter 13. Biofuels-economy, environment and sustainability. InTech; 2013.
[76] Alvim DS, Gatti LV, Corrêa SM, Chiquetto JB, de Souza Rossatti C, Pretto A, Dos Santos MH, Yamazaki A, Orlando JP, Santos GM. Main ozone-forming VOCs in the city of Sao Paulo: observations, modelling and impacts. Air Qual Atmos Health 2017;10(4):421–35.

[77] Alvim DS, Gatti LV, Corrêa SM, Chiquetto JB, Santos GM, de Souza Rossatti C, Figueroa SN, Pendharkar J, Nobre P. Determining VOCs reactivity for ozone forming potential in the megacity of São Paulo. Aerosol Air Qual Res 2018;18(9):2460–74.
[78] IPCC, 2006a. Intergovernmental Panel on Climate Change, 2006a. Guidelines for national greenhouse gas inventories, volume 2 energy.
[79] IPCC, 2006b. Intergovernmental Panel on Climate Change, 2006b. Guidelines for national greenhouse gas inventories, volume 5 waste.
[80] IPCC, 2007, Intergovernmental Panel on Climate Change, 2007. Fourth Assessment Report http://www.ipcc.ch/S.
[81] GEE, 2015 - Inventário de emissões de Gases de Efeito Estufa do Estado do Rio de Janeiro: ano base 2015: resumo técnico/Secretaria do Ambiente. – Rio de Janeiro, 2017. 48 p.: il. col. (download - http://www.centroclima.coppe.ufrj.br/index.php/br/estudos-e-projetos/encerrados/36-2017).
[82] Cepeda MA, Monteiro GP, de Oliveira Moita JV, Caprace JD. Estimating ship emissions based on AIS big data for the port of Rio de Janeiro. Proceedings of 17th Conference on Computer and IT Applications in the Maritime Industries 2018;1(1):189–203.
[83] Amarante OAC, SILVA FD, Rios Filho LG. Atlas eólico do Estado do Rio de Janeiro. Rio de Janeiro. Available at: http://www.cresesb.cepel.br/; 2002.